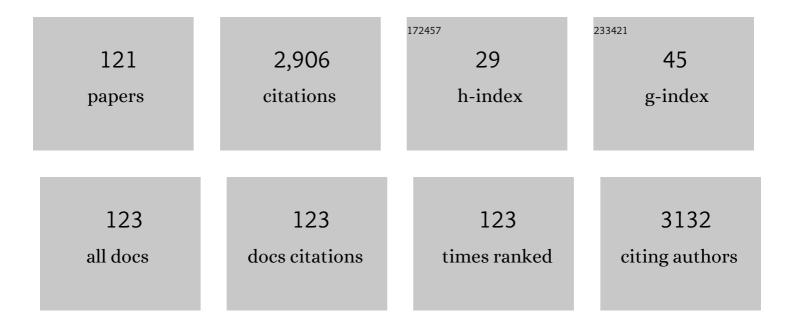
List of Publications by Year in descending order

Source: https://exaly.com/author-pdf/758240/publications.pdf Version: 2024-02-01



#	Article	IF	CITATIONS
1	Emergence of Uranium as a Distinct Metal Center for Building Intrinsic Xâ€ray Scintillators. Angewandte Chemie - International Edition, 2018, 57, 7883-7887.	13.8	198
2	Rational Design of Highâ€Performance Bilayer Solar Evaporator by Using Waste Polyesterâ€Derived Porous Carbon oated Wood. Energy and Environmental Materials, 2022, 5, 617-626.	12.8	116
3	High-performance solar-driven interfacial evaporation through molecular design of antibacterial, biomass-derived hydrogels. Journal of Colloid and Interface Science, 2022, 608, 840-852.	9.4	97
4	Molecular Properties of Flammulina velutipes Polysaccharide–Whey Protein Isolate (WPI) Complexes via Noncovalent Interactions. Foods, 2021, 10, 1.	4.3	90
5	Direct Radiation Detection by a Semiconductive Metal–Organic Framework. Journal of the American Chemical Society, 2019, 141, 8030-8034.	13.7	85
6	Biosorption of uranium on Bacillus sp. dwc-2: preliminary investigation on mechanism. Journal of Environmental Radioactivity, 2014, 135, 6-12.	1.7	77
7	Identification of novel DPP–IV inhibitory peptides from Atlantic salmon (Salmo salar) skin. Food Research International, 2020, 133, 109161.	6.2	69
8	Protective effects of Astragalin on spermatogenesis in streptozotocin-induced diabetes in male mice by improving antioxidant activity and inhibiting inflammation. Biomedicine and Pharmacotherapy, 2019, 110, 561-570.	5.6	64
9	Synthesis of amidoximated graphene oxide nanoribbons from unzipping of multiwalled carbon nanotubes for selective separation of uranium(<scp>vi</scp>). RSC Advances, 2015, 5, 89309-89318.	3.6	60
10	Selfâ€Floating Efficient Solar Steam Generators Constructed Using Superâ€Hydrophilic N,O Dualâ€Doped Carbon Foams from Waste Polyester. Energy and Environmental Materials, 2022, 5, 1204-1213.	12.8	55
11	Competition/Cooperation between Humic Acid and Graphene Oxide in Uranyl Adsorption Implicated by Molecular Dynamics Simulations. Environmental Science & Technology, 2019, 53, 5102-5110.	10.0	53
12	Controllable synthesis of N/Co-doped carbon from metal–organic frameworks for integrated solar vapor generation and advanced oxidation processes. Journal of Materials Chemistry A, 2022, 10, 13378-13392.	10.3	52
13	A capillary biosensor for rapid detection of Salmonella using Fe-nanocluster amplification and smart phone imaging. Biosensors and Bioelectronics, 2019, 127, 142-149.	10.1	51
14	IbSIMT1, a novel salt-induced methyltransferase gene from Ipomoea batatas, is involved in salt tolerance. Plant Cell, Tissue and Organ Culture, 2015, 120, 701-715.	2.3	50
15	The In Vitro Protective Role of Bovine Lactoferrin on Intestinal Epithelial Barrier. Molecules, 2019, 24, 148.	3.8	50
16	Bioaccumulation characterization of uranium by a novel Streptomyces sporoverrucosus dwc-3. Journal of Environmental Sciences, 2016, 41, 162-171.	6.1	46
17	A crystalline covalent organic framework embedded with a crystalline supramolecular organic framework for efficient iodine capture. Journal of Materials Chemistry A, 2021, 9, 16961-16966.	10.3	43
18	Inhibition of cell migration by ouabain in the A549 human lung cancer cell line. Oncology Letters, 2013, 6, 475-479.	1.8	42

#	Article	lF	CITATIONS
19	An ultrasensitive biosensor for colorimetric detection of Salmonella in large-volume sample using magnetic grid separation and platinum loaded zeolitic imidazolate Framework-8 nanocatalysts. Biosensors and Bioelectronics, 2020, 150, 111862.	10.1	40
20	Neuroadaptive integral robust control of visual quadrotor for tracking a moving object. Mechanical Systems and Signal Processing, 2020, 136, 106513.	8.0	39
21	Synthesis of cyclopropane fatty acid and its effect on freeze-drying survival of Lactobacillus bulgaricus L2 at different growth conditions. World Journal of Microbiology and Biotechnology, 2009, 25, 1659-1665.	3.6	38
22	Characteristics of uranium biosorption from aqueous solutions on fungus Pleurotus ostreatus. Environmental Science and Pollution Research, 2016, 23, 24846-24856.	5.3	36
23	A simple and convenient method for production of 89Zr with high purity. Applied Radiation and Isotopes, 2016, 118, 326-330.	1.5	34
24	Dynamics of Humic Acid and Its Interaction with Uranyl in the Presence of Hydrophobic Surface Implicated by Molecular Dynamics Simulations. Environmental Science & Technology, 2016, 50, 11121-11128.	10.0	34
25	Emergence of Uranium as a Distinct Metal Center for Building Intrinsic Xâ€ray Scintillators. Angewandte Chemie, 2018, 130, 8009-8013.	2.0	32
26	Facile and Efficient Decontamination of Thorium from Rare Earths Based on Selective Selenite Crystallization. Inorganic Chemistry, 2018, 57, 1880-1887.	4.0	32
27	Detection of Canopy Chlorophyll Content of Corn Based on Continuous Wavelet Transform Analysis. Remote Sensing, 2020, 12, 2741.	4.0	32
28	High-performance salt-resistant solar interfacial evaporation by flexible robust porous carbon/pulp fiber membrane. Science China Materials, 2022, 65, 201-212.	6.3	32
29	Microbial reduction of uranium (VI) by Bacillus sp. dwc-2: A macroscopic and spectroscopic study. Journal of Environmental Sciences, 2017, 53, 9-15.	6.1	31
30	Calcium antagonistic effects of Chinese crude drugs: Preliminary investigation and evaluation by 45Ca. Applied Radiation and Isotopes, 2005, 63, 151-155.	1.5	30
31	Biosorption behavior and mechanism of cesium-137 on Rhodosporidium fluviale strain UA2 isolated from cesium solution. Journal of Environmental Radioactivity, 2014, 134, 6-13.	1.7	30
32	Releasing Metal-Coordination Capacity of Cucurbit[6]uril Macrocycle in Pseudorotaxane Ligands for the Construction of Interwoven Uranyl–Rotaxane Coordination Polymers. Inorganic Chemistry, 2018, 57, 13513-13523.	4.0	29
33	Sorption of selenite on Tamusu clay in simulated groundwater with high salinity under aerobic/anaerobic conditions. Journal of Environmental Radioactivity, 2019, 203, 210-219.	1.7	29
34	Exopolysaccharide Produced by Lactobacillus Plantarum Induces Maturation of Dendritic Cells in BALB/c Mice. PLoS ONE, 2015, 10, e0143743.	2.5	27
35	Modelâ€assisted extended state observer and dynamic surface control–based trajectory tracking for quadrotors via outputâ€feedback mechanism. International Journal of Robust and Nonlinear Control, 2018, 28, 2404-2423.	3.7	27
36	Growth Stages Classification of Potato Crop Based on Analysis of Spectral Response and Variables Optimization. Sensors, 2020, 20, 3995.	3.8	27

#	Article	IF	CITATIONS
37	A radiopharmaceutical [89Zr]Zr-DFO-nimotuzumab for immunoPET with epidermal growth factor receptor expression in vivo. Nuclear Medicine and Biology, 2019, 70, 23-31.	0.6	25
38	Analysis of Chlorophyll Concentration in Potato Crop by Coupling Continuous Wavelet Transform and Spectral Variable Optimization. Remote Sensing, 2020, 12, 2826.	4.0	25
39	High-performance solar vapor generation by sustainable biomimetic snake-scale-like porous carbon. Sustainable Energy and Fuels, 2020, 4, 5522-5532.	4.9	25
40	Lightweight and Wearable Xâ€Ray Shielding Material with Biological Structure for Low Secondary Radiation and Metabolic Saving Performance. Advanced Materials Technologies, 2020, 5, 2000240.	5.8	25
41	Secondary Grain Growth in Organic–Inorganic Perovskite Films with Ethylamine Hydrochloride Additives for Highly Efficient Solar Cells. ACS Applied Materials & Interfaces, 2020, 12, 20026-20034.	8.0	25
42	Uranium(VI) sorption on graphene oxide nanoribbons derived from unzipping of multiwalled carbon nanotubes. Journal of Radioanalytical and Nuclear Chemistry, 2015, 304, 1329-1337.	1.5	24
43	Integrated transcriptome and proteome analysis provides insight into chilling-induced dormancy breaking in Chimonanthus praecox. Horticulture Research, 2020, 7, 198.	6.3	24
44	Inhibitory mechanism of phthalate esters on Karenia brevis. Chemosphere, 2016, 155, 498-508.	8.2	23
45	Preparation and characterization of continuous SiZrOC fibers by polyvinyl pyrrolidone-assisted sol–gel process. Journal of Materials Science, 2016, 51, 1418-1427.	3.7	23
46	Fate of four phthalate esters with presence of Karenia brevis: Uptake and biodegradation. Aquatic Toxicology, 2019, 206, 81-90.	4.0	23
47	Biosorption behavior and mechanism of thorium on Streptomyces sporoverrucosus dwc-3. Journal of Radioanalytical and Nuclear Chemistry, 2014, 301, 237-245.	1.5	22
48	Effect of humic acid on uranium(VI) retention and transport through quartz columns with varying pH and anion type. Journal of Environmental Radioactivity, 2017, 177, 142-150.	1.7	22
49	Biosorption of 241Am by Saccharomyces cerevisiae: Preliminary investigation on mechanism. Journal of Radioanalytical and Nuclear Chemistry, 2008, 275, 173-180.	1.5	21
50	Interface Engineering of 2D/3D Perovskite Heterojunction Improves Photovoltaic Efficiency and Stability. Solar Rrl, 2021, 5, 2100072.	5.8	21
51	Mild Periodic Acid Flux and Hydrothermal Methods for the Synthesis of Crystalline f-Element-Bearing Iodate Compounds. Inorganic Chemistry, 2017, 56, 13041-13050.	4.0	20
52	Flexible surface-supported MOF membrane via a convenient approach for efficient iodine adsorption. Journal of Radioanalytical and Nuclear Chemistry, 2020, 324, 1167-1177.	1.5	20
53	Functionalized hydrothermal carbon derived from waste pomelo peel as solid-phase extractant for the removal of uranyl from aqueous solution. Environmental Science and Pollution Research, 2017, 24, 22321-22331.	5.3	19
54	Integral Barrier Lyapunov Function Based Saturated Dynamic Surface Control for Vision-Based Quadrotors via Back-Stepping. IEEE Access, 2018, 6, 63292-63304.	4.2	19

#	Article	IF	CITATIONS
55	The Functional Role of Lactoferrin in Intestine Mucosal Immune System and Inflammatory Bowel Disease. Frontiers in Nutrition, 2021, 8, 759507.	3.7	18
56	Astatine-211 labeling of protein using TCP as a bi-functional linker: synthesis and preliminary evaluation in vivo and in vitro. Journal of Radioanalytical and Nuclear Chemistry, 2011, 288, 71-77.	1.5	17
57	Continuous sol–gel derived SiOC/HfO ₂ fibers with high strength. RSC Advances, 2015, 5, 35026-35032.	3.6	17
58	Intriguing substitution of conducting layer triggered enhancement of thermoelectric performance in misfit-layered (SnS)1.2(TiS2)2. Applied Physics Letters, 2017, 110, .	3.3	17
59	Exopolysaccharide Produced by <i>Lactobacillus casei</i> Promotes the Differentiation of CD4 ⁺ T Cells into Th17 Cells in BALB/c Mouse Peyer's Patches in Vivo and in Vitro. Journal of Agricultural and Food Chemistry, 2020, 68, 2664-2672.	5.2	17
60	A synergistic photothermal and photocatalytic membrane for efficient solar-driven contaminated water treatment. Sustainable Energy and Fuels, 2021, 5, 5627-5637.	4.9	17
61	Mechanism of thorium biosorption by the cells of the soil fungal isolate Geotrichum sp. dwc-1. Radiochimica Acta, 2014, 102, 175-184.	1.2	16
62	Characterization of uranium bioaccumulation on a fungal isolate Geotrichum sp. dwc-1 as investigated by FTIR, TEM and XPS. Journal of Radioanalytical and Nuclear Chemistry, 2016, 310, 165-175.	1.5	16
63	Effect of Lactoferrin on the Expression Profiles of Long Non-coding RNA during Osteogenic Differentiation of Bone Marrow Mesenchymal Stem Cells. International Journal of Molecular Sciences, 2019, 20, 4834.	4.1	16
64	The influence of humic substances on uranium biomineralization induced by Bacillus sp. dwc-2. Journal of Environmental Radioactivity, 2019, 197, 23-29.	1.7	16
65	Preparation and Properties of <i>Rhizopus oryzae</i> Lipase Immobilized Using an Adsorption-Crosslinking Method. International Journal of Food Properties, 2016, 19, 1776-1785.	3.0	15
66	Detection of chlorophyll content in growth potato based on spectral variable analysis. Spectroscopy Letters, 2020, 53, 476-488.	1.0	15
67	Substitutional Disorder of SeO ₃ ^{2–} /IO ₃ [–] in the Crystalline Solid Matrix: Insights into the Fate of Radionuclides ⁷⁹ Se and ¹²⁹ I in the Environment. Inorganic Chemistry, 2017, 56, 3702-3708.	4.0	14
68	One-step labelling of a novel small-molecule peptide with astatine-211: preliminary evaluation in vitro and in vivo. Journal of Radioanalytical and Nuclear Chemistry, 2018, 316, 451-456.	1.5	14
69	MnO2-loaded microorganism-derived carbon for U(VI) adsorption from aqueous solution. Environmental Science and Pollution Research, 2019, 26, 3697-3705.	5.3	14
70	Attitude restricted back-stepping anti-disturbance control for vision based quadrotors with visibility constraint. ISA Transactions, 2020, 100, 109-125.	5.7	14
71	Covalent Organic Framework Membrane with Turing Structures for Deacidification of Highly Acidic Solutions. Advanced Functional Materials, 2022, 32, 2108178.	14.9	14
72	Humulus scandens-Derived Biochars for the Effective Removal of Heavy Metal Ions: Isotherm/Kinetic Study, Column Adsorption and Mechanism Investigation. Nanomaterials, 2021, 11, 3255.	4.1	14

#	Article	IF	CITATIONS
73	Extraction of Trivalent Europium and Americium from Nitric Acid Solution with Bisdiglycolamides. Separation Science and Technology, 2015, 50, 1384-1393.	2.5	13
74	Different magnetic responses observed in Coll4, Coll3 and Coll1-based MOFs. Dalton Transactions, 2016, 45, 11864-11875.	3.3	13
75	The effect of U speciation in cultivation solution on the uptake of U by variant Sedum alfredii. Environmental Science and Pollution Research, 2016, 23, 9964-9971.	5.3	13
76	Removal of Co(II) from aqueous solution with functionalized metal–organic frameworks (MOFs) composite. Journal of Radioanalytical and Nuclear Chemistry, 2019, 322, 827-838.	1.5	13
77	Inorganic X-ray Scintillators Based on a Previously Unnoticed but Intrinsically Advantageous Metal Center. Inorganic Chemistry, 2019, 58, 2807-2812.	4.0	13
78	Preliminary investigation on biosorption mechanism of 241Am by Rhizopus arrhizus. Journal of Radioanalytical and Nuclear Chemistry, 2008, 277, 329-336.	1.5	12
79	Extraction and thermodynamic behavior of U(VI) and Th(IV) from nitric acid solution with tri-isoamyl phosphate. Journal of Radioanalytical and Nuclear Chemistry, 2013, 298, 651-656.	1.5	12
80	Kinked-Helix Actinide Polyrotaxanes from Weakly Bound Pseudorotaxane Linkers with Variable Conformations. Inorganic Chemistry, 2020, 59, 4058-4067.	4.0	12
81	Astatine-211 labeling of insulin: Synthesis and preliminary evaluation in vivo and in vitro. Journal of Radioanalytical and Nuclear Chemistry, 2007, 272, 85-90.	1.5	11
82	An investigation on the subcellular distribution and compartmentalization of uranium in Phaseolus vulgaris L Journal of Radioanalytical and Nuclear Chemistry, 2014, 299, 1351-1357.	1.5	11
83	Sorption of241Am by Aspergillus niger spore and hyphae. Journal of Radioanalytical and Nuclear Chemistry, 2004, 260, 659-663.	1.5	10
84	Radioiodination of insulin using N-succinimidyl 5-(tributylstannyl)-3-pyridine-carboxylate (SPC) as a bi-functional linker: Synthesis and biodistribution in mice . Journal of Radioanalytical and Nuclear Chemistry, 2006, 268, 205-210.	1.5	10
85	A study on the preparation and some functional properties of a cross-linked casein-gelatin composite by a microbial transglutaminase. International Journal of Food Science and Technology, 2011, 46, 2641-2647.	2.7	10
86	Monitoring binding affinity between drug and α1-acid glycoprotein in real time by Venturi easy ambient sonic-spray ionization mass spectrometry. Talanta, 2015, 143, 240-244.	5.5	10
87	Comparing the composition and trend of fatty acid in human milk with bovine milk and infant formula in northeast region of China. CYTA - Journal of Food, 2016, 14, 632-638.	1.9	10
88	A novel metal–organic framework derived carbon nanoflower with effective electromagnetic microwave absorption and high-performance electrochemical energy storage properties. Chemical Communications, 2021, 57, 2539-2542.	4.1	10
89	Comparison Between Phase Behavior of Gemini Imidazoliums and Monomeric Ionic Liquid Surfactants in W/O Microemulsion Systems. Journal of Dispersion Science and Technology, 2015, 36, 129-135.	2.4	9
90	Desired compensation RISE-based IBVS control of quadrotors for tracking a moving target. Nonlinear Dynamics, 2019, 95, 2605-2624.	5.2	9

#	Article	IF	CITATIONS
91	Electroreduction-based Tb extraction from Tb4O7 on different substrates: understanding Al–Tb alloy formation mechanism in LiCl–KCl melt. RSC Advances, 2015, 5, 69134-69142.	3.6	8
92	Kinetics process of Tb(III)/Tb couple at liquid Zn electrode and thermodynamic properties of Tb-Zn alloys formation. Science China Chemistry, 2017, 60, 813-821.	8.2	8
93	Release of dipeptidyl peptidase IV inhibitory peptides from salmon (<i>Salmosalar</i>) skin collagen based on digestion–intestinal absorption <i>invitro</i> . International Journal of Food Science and Technology, 2021, 56, 3507-3518.	2.7	8
94	Upcycling Waste Polyethylene into Carbon Nanomaterial via a Carbonâ€Grownâ€onâ€Carbon Strategy. Macromolecular Rapid Communications, 2022, 43, e2100835.	3.9	8
95	Preparation and preliminary evaluation of 211At-labeled amidobisphophonates. Journal of Radioanalytical and Nuclear Chemistry, 2010, 283, 329-335.	1.5	7
96	Study of ultrahigh-purity copper billets refined by vacuum melting and directional solidification. Rare Metals, 2011, 30, 304-309.	7.1	7
97	Urinary Metabolic Profiling via LC-MS/MS Reveals Impact of Bovine Lactoferrin on Bone Formation in Growing SD Rats. Nutrients, 2020, 12, 1116.	4.1	7
98	Effect of MnCl2 deposition content on the textural properties of activated alumina and its elution performance for hydrogen isotopes. Adsorption, 2017, 23, 13-18.	3.0	6
99	Indium-111 labeled bleomycin for targeting diagnosis and therapy of liver tumor: optimized preparation, biodistribution and SPECT imaging with xenograft models. Journal of Radioanalytical and Nuclear Chemistry, 2019, 322, 545-551.	1.5	6
100	Comparative proteome analysis of Streptomyces mobaraensis under MgCl2 stress shows proteins modulating differentiation and transglutaminase biosynthesis. Food Research International, 2019, 121, 622-632.	6.2	6
101	Sorption of cesium on Tamusu clay in synthetic groundwater with high ionic strength. Radiochimica Acta, 2020, 108, 287-296.	1.2	6
102	Reconstruction of the Diaminopimelic Acid Pathway to Promote L-lysine Production in Corynebacterium glutamicum. International Journal of Molecular Sciences, 2021, 22, 9065.	4.1	6
103	The Complete Mitochondrial Genomes of Four Species in the Subfamily Limenitidinae (Lepidoptera,) Tj ETQq1 1 (0.784314 2.2	rg&T /Overlo
104	Determining <scp>N</scp> eu5 <scp>A</scp> c in infant formula with ultraâ€performance liquid chromatography–tandem massÂspectrometry. International Journal of Dairy Technology, 2015, 68, 166-173.	2.8	5
105	An Insight into Adaptive Deformation of Rigid Cucurbit[6]uril Host in Symmetric [2]Pseudorotaxanes. European Journal of Organic Chemistry, 2018, 2018, 4426-4430.	2.4	5
106	Construction and Preclinical Evaluation of 211At Labeled Anti-mesothelin Antibodies as Potential Targeted Alpha Therapy Drugs. Journal of Radiation Research, 2020, 61, 684-690.	1.6	5
107	Temperatureâ€induced mutagenesisâ€based adaptive evolution of Bacillus amyloliquefaciens for improving the production efficiency of menaquinoneâ€7 from starch. Journal of Chemical Technology and Biotechnology, 2021, 96, 1040-1048.	3.2	5
108	Astatine-211 labelled a small molecule peptide: specific cell killing <i>in vitro</i> and targeted therapy in a nude-mouse model. Radiochimica Acta, 2021, 109, 119-126.	1.2	5

#	Article	IF	CITATIONS
109	Green Synthesis of Carbon Nitrideâ€Based Conjugated Copolymer for Efficient Photocatalytic Degradation of Tetracycline. Macromolecular Rapid Communications, 2022, 43, e2200043.	3.9	5
110	Extraction kinetics of Uranium(VI) and Thorium(IV) with Tri-iso-amyl phosphate from nitric acid using a Lewis Cell. Journal of Radioanalytical and Nuclear Chemistry, 2014, 302, 1069-1076.	1.5	4
111	Adsorption and migration of 241Am in aerated zone soil. Journal of Radioanalytical and Nuclear Chemistry, 2007, 274, 593-601.	1.5	3
112	Phase and rietveld refinement of pyrochlore Gd2Zr2O7 used for immobilization of Pu (IV). Journal Wuhan University of Technology, Materials Science Edition, 2014, 29, 233-236.	1.0	3
113	A novel orally available Syk/Src/Jak2 inhibitor, SKLB-850, showed potent anti-tumor activities in B cell lymphoma (BCL) models. Oncotarget, 2017, 8, 111495-111507.	1.8	3
114	A Theoretical Model for Predicting and Optimizing In Vitro Screening of Potential Targeted Alpha-Particle Therapy Drugs. Radiation Research, 2019, 191, 475.	1.5	3
115	Superconductivity induced by U doping in the SmFeAsO system. Physical Review B, 2013, 87, .	3.2	2
116	Phase and structure in the system Gd2â^'x Eu x Zr2O7 (0.0 ⩽ x ⩽ 2.0). Journal Wuhan University of Technology, Materials Science Edition, 2014, 29, 1-4.	1.0	2
117	Innenrücktitelbild: Emergence of Uranium as a Distinct Metal Center for Building Intrinsic X-ray Scintillators (Angew. Chem. 26/2018). Angewandte Chemie, 2018, 130, 8031-8031.	2.0	1
118	A Strong Robust wavelet-based watermarking technology for copyright protection. , 2012, , .		0
119	Highly selective extraction of Pd(II) with 5-octyloxymethyl-7-bromo-8-quinolinol from acidic solution. Journal of Radioanalytical and Nuclear Chemistry, 2017, 314, 59-67.	1.5	0
120	A Cross-layer Routing with Interference Constraint for VANETs. , 2018, , .		0
121	Production of 98Tc with high isotopic purity. Applied Radiation and Isotopes, 2020, 160, 109133.	1.5	0